2022-02-01

Occurrence and chemical characteristics of microplastic paint flakes in the North Atlantic Ocean

Turner, Andrew

10.1016/j.scitotenv.2021.150375
Science of The Total Environment
Elsevier BV

Occurrence and chemical characteristics of microplastic paint flakes in the North Atlantic Ocean

Andrew Turner[a*], Clare Ostle[b], Marianne Wootton[b]

*[a]*School of Geography, Earth and Environmental Sciences*
University of Plymouth
Drake Circus
Plymouth PL4 8AA, UK

[b] *The Marine Biological Association (MBA),*
The Laboratory
Citadel Hill
Plymouth PL1 2PB, UK

*Corresponding author. e-mail: aturner@plymouth.ac.uk

Accepted 12th September 2021

https://doi.org/10.1016/j.scitotenv.2021.150375

Abstract

Non-fibrous microplastics sampled by the Continuous Plankton Recorder (CPR) Survey throughout the North Atlantic Ocean during 2018 have been recorded and a selection (*n* = 17, or 16.7 % of non-fibrous particles collected) physically and chemically characterized. The average abundance of flakes captured by the plankton silks and detectable by microscopy was estimated to be around 0.01 m^{-3}, with the highest concentrations evident in shelf seas of northwest Europe. Amongst the samples analysed, median size was 180 μm and, based on visible properties (e.g., brittleness, layering) and infra-red spectra, all but one were identified as flakes of paint. Semi-quantitative analysis by energy-dispersive X-ray fluorescence spectrometry with a collimated beam revealed that six flakes from European shelf seas were Cu-based antifouling formulations (without evidence of organo-Sn compounds), and five with a broader geographical distribution were Pb-based formulations of likely marine origin. Other elements regularly detected included Cr, Fe, Ti and Zn that were present in pigments or as contaminants from the underlying substrate. After fibres, paint flakes appear to be the most abundant type of microplastic in the oceans that, because of the abundance and mobility of metallic additives, deserve closer scientific attention.

Keywords: energy-dispersive XRF; paint flakes; microplastics; pigments; Atlantic Ocean; metals

Introduction

Microplastics as marine contaminants have come under intense scientific scrutiny over the past two decades (Ng and Obbard, 2006; do Sul et al., 2013; Ruiz-Orejon et al., 2016; Burkhardt-Holm and N'Guyen, 2019; Tanhua et al., 2020). Primary and secondary microplastics of sub-mm dimensions are derived from an array of land-based and offshore sources and encompass a variety of shapes (e.g., fibres, fragments, flakes, films, pellets), materials (or polymers), structures (e.g., rigid, flexible, foamed) and properties (e.g., density, crystallinity, hardness). Microplastics may also exhibit different surface morphologies depending on the polymer and its structure and any impacts of weathering and chemical- and bio-fouling (Richard et al., 2019; Liu et al., 2020).

One type of microplastic that has received relatively little attention is microscopic paint flakes that are generated by weathering or abrasion of coatings. Paint particles are typically more angular, brittle and layered than most other types of microplastic because of a relatively low polymer content (and relatively high functional additive and filler content) and the application of multiple coatings to a substrate. These properties result in a physico-chemical composition that is typically much more heterogeneous than other plastics and one that more readily enables the migration of additives from the matrix (Turner, 2021). Significantly, many contemporary and historical paint additives are potentially harmful because they have antifouling or anti-corrosive properties (del Amo et al., 2002; Takahashi et al., 2012).

In the recent literature, paint flakes have been identified amongst microplastics sampled in the marine environment and from the digestive tracts of marine animals

(Cardoza et al., 2018; Aliabad et al., 2019; Herrera et al., 2019; Lacerda et al., 2019), with some studies suggesting that paint might be the dominant form of microdebris at or near the sea surface (Lima et al., 2014; Kang et al., 2015). It is generally assumed or implied that paint particles are derived from shipping activities, although this is difficult to establish without chemical characterisation of the material by, for example, pyrolysis-gas chromatography-mass spectrometry (Dibke et al., 2021; Lee et al., 2021).

An alternative means of non-destructively characterising microscopic paint flakes is to determine the elemental (e.g., pigment) content of samples by energy-dispersive X-ray techniques. X-ray spectroscopy coupled with scanning electron microscopy (EDS-SEM) can be used to semi-quantitatively characterise elements of relatively low secondary X-ray energies at the 0.1% level, but the higher excitation energies and larger irradiation areas make X-ray fluorescence (XRF) spectroscopy more suited to analysing heavier metals at lower concentrations in more inhomogeneous samples.

In the present study, microplastics retrieved from plankton trawls towed throughout different regions of the North Atlantic region are examined to determine the presence and significance of microscopic paint flakes, and information on the chemical characteristics and origin of the particles is gained by Fourier transform infrared (FTIR) and energy-dispersive XRF analyses. The more general capability of the latter technique to quantify the metal (hence, pigment) content of microplastic paint flakes is also explored in a series of tests in which paint particle diameters are successively reduced.

Materials and methods

Sampling and the CPR

Microplastic samples were collected by analysts recording and cataloguing the contents of silks as part of the Continuous Plankton Recorder (CPR) Survey at the Marine Biological Association. The majority of microplastics identified within the CPR Survey in the past have been fibrous in nature, partly because of their ease of identification (Thompson et al., 2004; Sadri, 2015). Here, however, analysts were instructed to record plastics that were non-fibrous (that is, fragments or flakes, and hereafter referred to as "flakes") during their routine examinations, and to retrieve selected samples for further characterisation.

The CPR is described comprehensively by Richardson et al. (2006). Briefly, the device itself is approximately 1 m in length and is towed behind commercial vessels throughout the North Atlantic and farther afield at a speed of up to 10 m s^{-1} and a depth of about 7 m. Seawater passes through a square aperture of 1.6 cm^2 and plankton (and microplastics) are filtered onto a slowly moving band of silk (270-μm mesh size) driven by a propeller-gearbox. The silk is covered with a second band of moving silk and the contents are spooled into a storage tank containing formalin. In the laboratory, the filtering silk is unwound and divided into sections representing 10 nautical miles of tow (equivalent to approximately 3 m^3 of water filtered), with the time and location of a section derived from the ship's route and speed and the rate of silk advance within the device. Sections of silk are examined on a mobile sliding glass stage housed inside a ventilated fume cupboard, using a binocular compound bright field microscope at 50 x and 500 x magnification coupled with a circular counting reticule measuring 2 mm and 0.295 mm in diameter, respectively (Sadri, 2015).

Larger planktonic organisms (and microplastics) are inspected under a lower magnification stereo dissecting microscope.

Although the CPR sampling method is described as semi-quantitative due to the relatively large mesh-size and small aperture, it captures a consistent fraction of particles within the water column (Richardson et al., 2006). Currently there is not a standardised NMBAQC (NE Atlantic Marine Biological Analytical Quality Control Scheme) protocol for microplastic enumeration. However, the skilled team of CPR analysts follow the OSPAR (Oslo-Paris Convention for the Protection of the Marine Environment of the North-East Atlantic) guidelines recording the size, shape and colour (Maes et al., 2017). Compared to a Manta net trawl (typically used for sampling microplastics), the CPR captures fewer particles when assessed by number of items. However, when standardised by the volume of water sampled, CPR samples and Manta trawl samples yield values that are not significantly different from each other (Sadri, 2015).

Microplastic analysis

Seventeen microplastic flakes from various tows conducted in different regions of the North Atlantic in 2018 (and mainly during late summer) were retrieved using a pair of stork-billed, fine-pointed forceps and placed in the centre of individual 47-mm diameter Whatman filter papers. Filters were folded twice and stored in petri dishes that were sealed with clear adhesive tape. Flakes were first examined and photographed while on their filter papers under a Nikon SMZ800 stereo-microscope in order to estimate particle size and observe any surface or structural features. Samples removed from their filters were subsequently characterised for chemical

composition by energy-dispersive XRF spectrometry and as described below, before the polymers were identified by FTIR spectroscopy. For FTIR analysis, flakes were clamped down on to the diamond crystal of a Bruker ALPHA Platinum attenuated total reflection QuickSnap A220/D-01 spectrometer. Measurements consisted of 16 scans in the range 4000 to 400 cm^{-1} and at a resolution of 4 cm^{-1}. Polymer identification involved a comparison of sample transmittance spectra with libraries of reference spectra and a hit quality criterion of > 70%.

XRF analysis

Analysis by energy-dispersive XRF was accomplished using a Niton XL3t 950 He GOLDD+ portable instrument housed, nose upwards, in a laboratory accessory stand and activated remotely by a laptop. With the aid of stainless steel precision tweezers, flakes were placed centrally over the detector window on 3.6 μm Mylar polyester film (Chemplex Industries, FL). Positioning was facilitated and particle size independently estimated with the aid of real-time imagery generated by a CCD camera within the detector window and a central, circular reticule of 3 mm that were both projected to the laptop via Niton software.

The XRF spectrometer was operated in a low density 'plastics' mode through a standard-less, fundamental parameters-based alpha coefficient correction model. This mode incorporates a thickness correction algorithm that accounts for the limited mass absorption of X-rays by polymers (flakes in the present study were assumed to have a thickness of 100 μm) and is able to detect 18 elements. The instrument's small-spot facility was employed throughout, whereby the primary X-ray beam is collimated to a diameter of 3 mm at the detector window (and defined by the circular reticule).

Secondary sample X-rays were counted for a period of 90 seconds, and during successive periods of irradiation at 50 kV and 40 μA (70 seconds) and 20 kV and 100 μA (20 seconds). Spectra were quantified by fundamental parameters to yield elemental concentrations on a dry weight basis (in mg kg^{-1}) and a counting error of 2σ (95% confidence).

XRF performance testing on microplastics

Given that the area of the flakes analysed by XRF (up to ~ 0.2 mm^2) are considerably smaller than the reticule and collimated beam area of the detector window (7.1 mm^2), the performance of the instrument was evaluated by determining elemental concentrations in plastics whose sizes encompassed this range. The results of tests undertaken on polyethylene and polyvinyl chloride cut to different sizes are reported elsewhere (Turner, 2017) while tests specifically performed on paint flakes are described as follows. Three samples of marine paint were acquired from the wooden hulls of two abandoned boats and the deck of a third abandoned boat in Hooe Lake (Plym estuary, SW Devon), and one sample of external decorative paint was sourced from a metal downpipe attached to the side wall of a domestic property in the city centre of Plymouth. Individual flakes that completely covered the reticule were analysed by XRF according to the operating conditions above before they were placed on Mylar film on a white benchtop and crushed with the handle of a pair of stainless steel tweezers. The tweezers were then used to pick out flakes of different sizes (n = 4 to 6) which were transferred, on the polyester film, to the steel base plate of the accessory stand. Each flake was analysed after carefully moving the film to align the central point of the sample into the centre of the reticule and detector window (Figure 1).

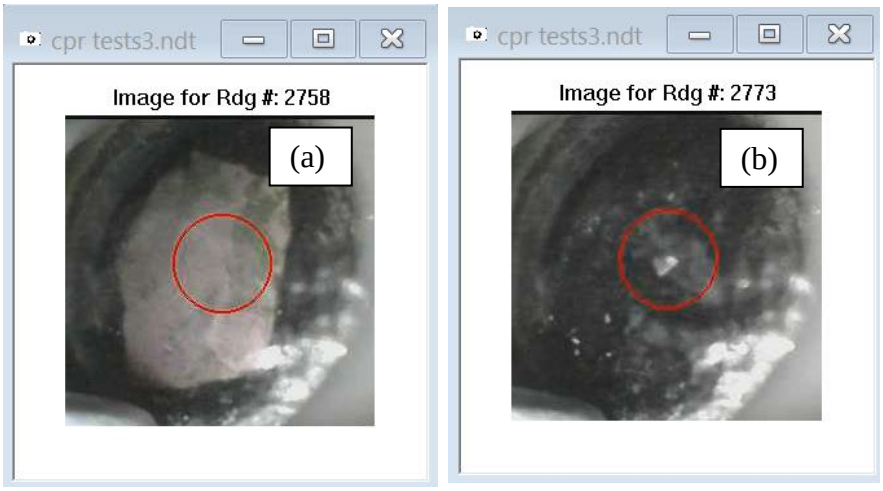

Figure 1: (a) A sample of boat paint on the XRF detector window and covering the area defined by the 3-mm reticule, and (b) a flake of about 700 μm in diameter generated by crushing the sample and centred in the 3-mm reticule.

Results and Discussion

Distribution of flakes

Figure 2 shows the routes of the CPR tows undertaken during 2018, along with the distribution of microplastic flakes that were recorded and flakes that were retrieved for characterisation. Flakes were observed in all tows and all regions sampled, but appeared to be more densely distributed around the shelf seas of northwest Europe. Overall, flakes were reported in about 2.8% (102) of all silks (3611) analysed. This compares with fibres or stands observed in 48.8% (1763) of silks.

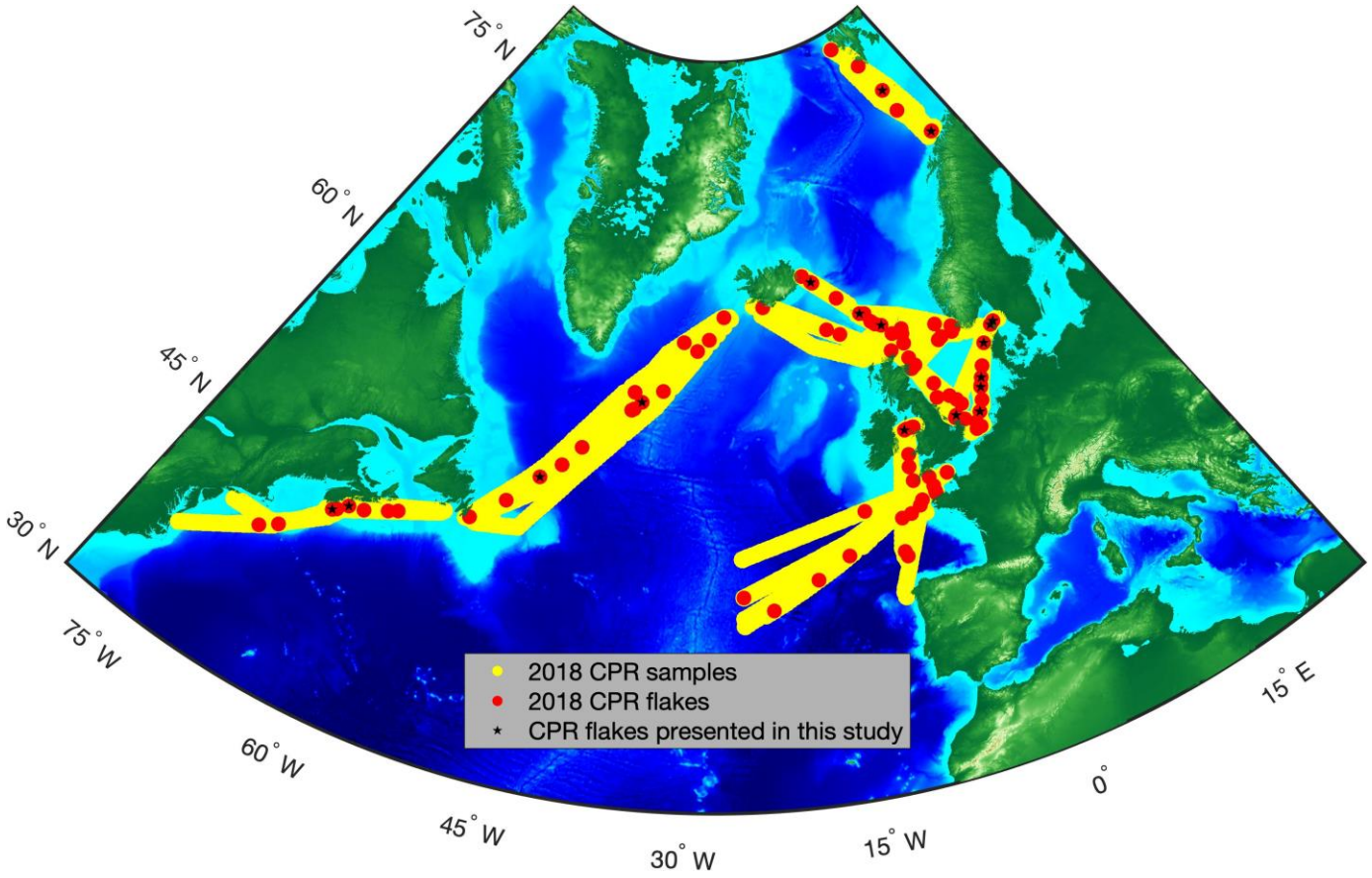

Figure 2: CPR samples in the North Atlantic for the year 2018 (overlapping and continuous yellow circles), locations where flakes were observed (red circles), and location of flakes analysed within this study (black stars).

Physical and polymeric characteristics of microplastic flakes

The locations and dates of the silks capturing the 17 flake samples characterised in the present study are shown in Table 1, along with the size of each particle (*d*, defined as the average of the largest and smallest diameter measured under the microscope) and, where recorded or evident, its colour. Median particle size was 180 μm, and the majority of particles were smaller than the mesh size of the silks (270 μm). This may be attributed to the variable aspect ratios of some flakes and, more generally, the gradual clogging of the mesh by gelatinous forms of phytoplankton and zooplankton that act to reduce the effective pore size of the silk (Richardson et al., 2006).

Table 1: Characteristics of the flake samples and locations and dates of collection (nd = not determined).

sample #	location	latitude	longitude	date	*d*, μm	type	colour	polymer
1	Labrador Sea	50.827	-46.888	Sep-18	1100	plastic	white	polyethylene terephthalate
2	Southern North Sea	53.247	1.127	Aug-18	230	paint	black	alkyd
3	Skagerrak	56.81	7.97	Aug-18	230	paint	silver	
4	Labrador Sea	57.067	-36.853	Aug-18	100	paint	black	
5	Barents Sea	74.64	15.837	Sep-18	90	paint	blue	alkyd
6	Skagerrak	57.635	9.853	Aug-18	210	paint	blue	epoxy
7	Southern North Sea	52.83	3.807	Aug-18	320	paint	pink-yellow	chlorinated rubber
8	Northern North Sea	60.628	-3.602	Sep-18	110	paint	nd	
9	Norwegian Sea	70.525	19.175	Apr-18	190	paint	nd	
10	Northeast Atlantic Ocean	61.828	-6.057	Aug-18	80	paint	black	
11	Central North Sea	54.837	5.737	Aug-18	230	paint	black	alkyd
12	Southern North Sea	54.267	5.14	Aug-18	160	paint	blue	
13	Irish Sea	53.517	-5.082	Aug-18	200	paint	blue	
14	Nova Scotia coast	44.14	-63.718	Aug-18	180	paint	blue	chlorinated rubber
15	Faroe-Iceland Rise	64.688	-12.063	Aug-18	70	paint	black	
16	Skagerrak	57.765	10.407	Aug-18	180	paint	blue	
17	Nova Scotia coast	43.4	-64.897	Aug-18	60	paint	blue	

Visual inspection of microplastic flakes and their response to handling with tweezers or clamping onto the diamond crystal of the FTIR allowed ready discrimination between thermoplastics and paints, with the latter distinctly brittle, more angular and irregular, and often multi-coloured and layered. Overall, and as indicated in Table 1, just one sample was thermoplastic (a white fragment of polyethylene terephthalate; # 1) and the remainder were paint flakes of various colours whose resins were alkyd-, epoxy- or chlorinated rubber-based. (Note that FTIR analysis of paints was incomplete as many samples were too small or fragile to withstand clamping on the crystal.)

XRF performance on microplastic paint flakes

Because the majority of microplastics retrieved from the North Atlantic region were paint-based, a critical component of the study was an evaluation of the response of the XRF spectrometer to paint particles of a comparable size. Figure 3 shows the concentration of different elements in four paints reported by the instrument as flake

size (d) is reduced from > 4 mm to < 250 μm. Thus, as the area occupied by the sample within the X-ray beam area was reduced, the counts registered by the detector decreased and the counting error (and detection limit) increased, but variable changes in elemental concentrations were returned by fundamental parameters that appeared to be sample- and element-specific. In many cases, a decreasing concentration occurs with a reduction in flake size that is either continuous (e.g. Cl and Fe in paint a, Sn in paints b and c, Cu and Zn in paint c) or occurs over a relatively small size range (e.g. Cr and Ti in paint a, Cu and Zn in paint b). In other cases, concentration appears to be independent of particle size (e.g. Fe and Pb in paint c, Ba, Pb, Zn in paint d) or increases with decreasing flake size (Ba in paints a and b). The precise causes of these different responses are unknown but could be related to variations in sample thickness, layering, binder content or absolute (true) elemental concentrations (measured at d > 4 mm), or to differences in secondary X-ray energies amongst the elements considered. Nevertheless, the results of this experiment reveal that no false positives arise as flake size is reduced, and that a semi-quantitative assessment of elemental composition of microscopic paint particles can be gained from the data returned and the trends observed in Figure 3.

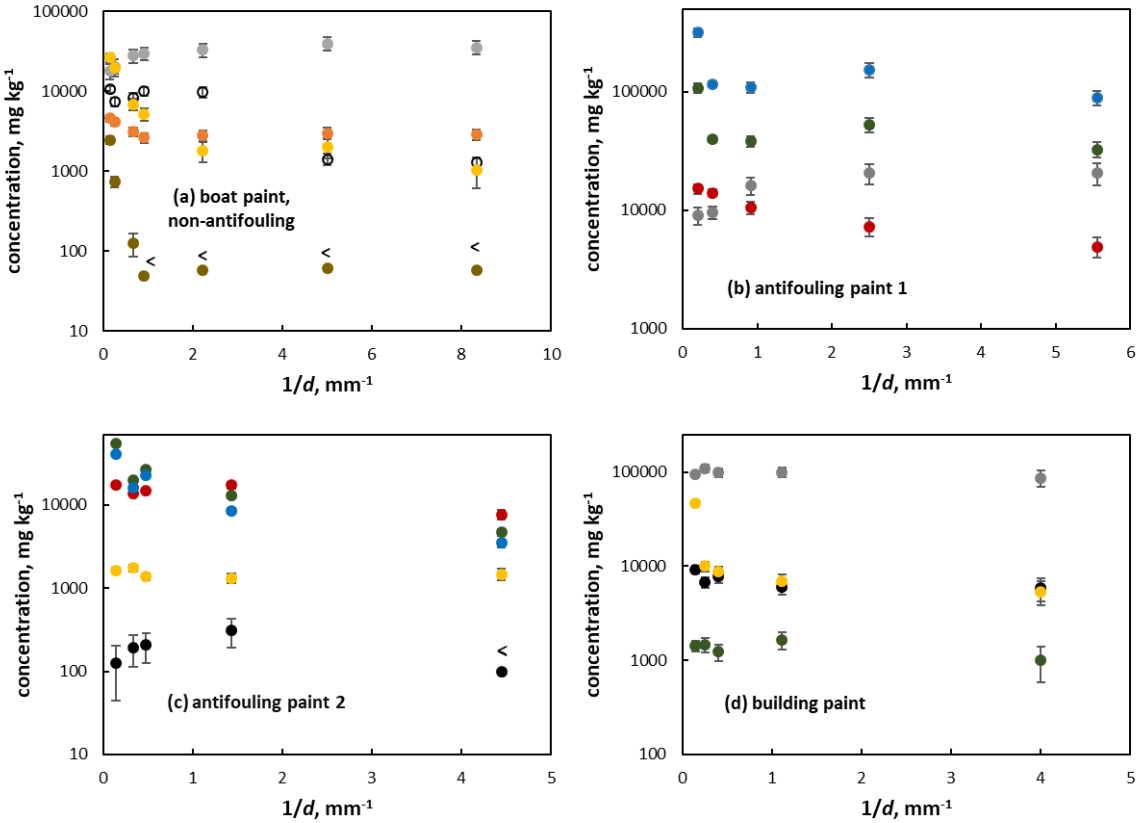

Figure 3: Concentrations of different elements returned by the XRF for four paints as flake size is reduced. Black = Pb; white = Ti; grey = Ba; green = Zn; blue = Cu; red = Sn; yellow = Fe; brown = Cr. Error bars represent two counting errors and < denotes not detected (and shown above the circle defining the size-specific detection limit).

Table 2: Results of XRF analysis of the microplastic flakes retrieved from the plankton silks. Concentrations (in bold) and detection limits (<) are in mg kg^{-1} and errors represent one standard deviation about the mean of five determinations undertaken at different positions and orientations within the 3-mm reticule (an asterisk denotes that the element was detected once amongst the replicates).

sample #	Ba	Cu	Cr	Fe	Pb	Sn	Ti	Zn
1	<2060	<56.4	<10.5	**93.9**	<46.8	**387**	**24500**	**87.2**
2	<10800	**3210**	<71.0	**2290**	<782	<1250	**1560**	**37400**
3	**7900***	<435	<42.6	**2850±810**	<206	<1210	**5440±413**	**2000±357**
4	<1770	<65.4	**41.9**	<74.7	<51.3	<278	<7.0	**139**
5	<18600	<956	<201	**31700**	<321	<1900	**71400**	<1030
6	**9770**	**1310**	**81.9**	**783**	**2670**	<875	<36.6	**6970**
7	<30000	**2060**	**121**	**4970**	**1220**	<421	**407**	**11400**
8	<2670	<114	**51.6**	**1220**	<84.5	<428	**1220**	<60.8
9	<11700	<548	<77.1	<808	<675	<1450	**8240**	<427
10	<3010	<130	**68.9**	<104	**4690**	<427	**30.0**	<95.1
11	**7510***	**824±265**	**617±78.6**	**3720±580**	**264***	<825	**3900±384**	**4550±620**
12	<1980	<75.2	**57.0**	<61.6	<51.6	<281	**7.5**	**972**
13	<1860	<58.6	**64.8**	<70.9	<55.2	<273	**23.4**	**218**
14	**1630**	<52.9	**33.3**	**426**	<27.5	<216	**2140**	**201**
15	**2320***	<86.0	**65.1±8.1**	<56.7	**17300±3650**	<261	**15.7±6.4**	<38.2
16	<4800	**6960**	**34.8**	**1060**	**29000**	<738	**31.3**	**5530**
17	<1800	<67.9	**56.1**	**161**	<42.9	<263	<6.6	**272**

Elemental profiles of microplastic flakes

The results of the XRF analysis of the microplastics retrieved from CPR tows in the North Atlantic are shown in Table 2. The data reveal the heterogeneity of the analyte concentrations and detection limits, both between elements and, for a given element, between samples, but a repeatability when the same sample is positioned differently that is usually better than 20%. Copper was detected in five paint samples at concentrations up to about 7000 mg kg^{-1}, with the information in Figure 3 suggesting that the true concentrations are likely to be significantly higher. Tin was only detected

in the thermoplastic sample and Pb was detected in six paints at concentrations that are variable but, according to Figure 3, are likely to be representative of true values. Chromium, Fe, Ti and Zn were detected in at least 11 samples with concentrations that are likely to be underestimates.

By comparison, Song et al. (2014) report concentrations of Cu, Fe, Pb and Zn of 29,000, 129,000, 73,000 and 17,000 mg kg^{-1}, respectively, in alkyd-based paint particles retrieved from the sea surface microlayer of coastal Korea. However, while the authors mention screening by "energy dispersive X-ray", no analytical details or constraints are provided and it is not clear whether concentrations represent an average of multiple samples or a single value arising from the analysis of a composite.

Table 3: Chemical characteristics of the paint flakes inferred from the information in Table 2. Filler and pigments are defined by concentrations exceeding 1000 mg kg^{-1}.

sample #	antifouling (Cu-based)	antifouling (TBT-based)	Ba filler	Fe pigment*	Pb pigment	Ti pigment	Zn pigment	Cr contamination
2	✔			✔		✔	✔	
3			✔	✔		✔	✔	
4								✔
5				✔		✔		
6	✔		✔		✔		✔	✔
7	✔			✔	✔		✔	✔
8				✔		✔		✔
9						✔		
10			✔		✔			✔
11	✔		✔	✔		✔	✔	✔
12								✔
13								✔
14			✔			✔		✔
15			✔		✔			✔
16	✔			✔	✔		✔	✔
17								✔

***It is suspected that Fe may also be present as a contaminant from the underlying (metallic) substrate.**

Types of microplastic paint flakes

Despite the uncertainties in the absolute metal concentrations reported here, coupled with variable analytical performances for different elements, the XRF data enable the broad chemical characteristics of the samples to be defined. Table 3 provides these characteristics for the paint particles, with the assumptions that a pigment or filler is present at a measured concentration of > 1000 mg kg^{-1} and the detection of Cu or Sn denotes an antifouling formulation based on compounds of Cu(I) and/or organotin. Note that presence of Cr is indicated as evidence of contamination by a Cr-based primer, and while Fe is included as a pigment, it is possible that the presence of this element also reflects contamination of the paint from corroded fragments of an underlying steel substrate.

Overall, we infer that six flakes of various colours and sampled from the shelf seas around northwest Europe are Cu-based antifouling flakes, with none of these samples exhibiting evidence of organotin-based antifouling agents. The highest concentrations of Zn were associated with detectable Cu, consistent with the common use of ZnO in Cu-based antifouling paints to improve performance and control erosion rates (Lindgren et al., 2018), but its presence in other samples suggests a wider use as a pigment in primers and topcoats. Five paint samples contained appreciable quantities of Pb, including three antifouling fragments (sample #s 6, 7, 16), that exhibited a broad distribution throughout the Atlantic. Lead associated with Cu may represent historical antifouling formulations in which inorganic or organo-lead compounds were

combined with Cu(I) (Cardarelli, 1976). However, it is more likely that the co-existence of these elements reflects distinct layers of a Cu-based antifouling formulation and a Pb-based anticorrosive steel primer (e.g., red lead). Sample #7 was sufficiently large and flat to analyse both faces by XRF and the results revealed distinctly different Cu:Pb concentration ratios (about 1.8 and 0.6). Clearly, X-ray attenuation is limited in paint of this thickness but the results suggest that layering was present in this case. More generally, it is suspected that the presence of small but variable quantities of Cr arise from the heterogeneous contamination of antifouling layers and other surface coatings by underlying basic chromated primers. Lead in the absence of Cu is consistent with the presence of leaded marine paint used above the water-line on wood or steel. Booher (1988) reports a geometric mean concentration of Pb in ship paints of 2500 mg kg^{-1} and, although Pb pigments have since been restricted, historical, extant formulations in various conditions are still likely to be present (Hall, 2006; Driscoll et al., 2016).

Origin and abundance of microplastic paint flakes

The implication of the discussion above is that the microscopic paint flakes retrieved from the plankton silks are derived from the hulls and other painted components of ships mobilised in the Atlantic region. Without information on the types of formulations employed on the commercial ships towing the CPR devices, it is not possible to ascertain whether samples were derived from these or other vessels. However, the visual and chemical characteristics of paint applied to the steel frame of a CPR device in storage (silver flakes with measurable Ba, Fe, Ti and Zn but no detectable Cr) suggest that one sample (# 3) was derived from material shed from the structure itself during sampling or silk retrieval. Inferences in the marine literature

regarding paint sources are varied, with some investigations matching sample colours and infra-red spectra to those of paint flaking from the trawl frame or research vessel (Bagaev et al., 2017; Lacerda et al., 2019) and other studies highlighting the importance of pre-existent paint particles (Song et al., 2014; Dibke et al., 2021).

Another potential source of paint samples trawled from the ocean is land-based inputs of weathered building and road coating particles via rivers, treated municipal sewage, untreated road runoff and the atmosphere. Estimates based on paint usage suggest that inputs to surface waters from this source should exceed inputs from marine paints (Hann et al., 2018). However, it is unlikely that particles as dense as dried paint formulations (up to about 3 g cm^{-3}; Ruble, 2002; Brockenbrough, 2009) and of the sizes typically trawled from the marine environment (a few hundred microns; Kang et al., 2015; Bagaev et al., 2017; Aliabad et al., 2019) are able to undergo long-range transportation in the surface of the ocean. For example, experiments performed by Soroldoni et al. (2018) showed that antifouling paint particles exceeding 1 mm in diameter settle in estuarine water according to density and size, and below 180 μm in diameter remain at the surface without agitation but settle after the surface tension is broken. In theory, therefore, and based on chemical characteristics of trawled particles reported here and elsewhere (Song et al., 2014; Dibke et al., 2021), shipping activities (including hull corrosion, and weathering and abrasion of ship paints above the waterline and paints applied to containers) would appear to be the dominant source of paint flakes in the ocean.

The data obtained in the present study allow us to estimate the absolute and relative abundance of paint flakes in the North Atlantic Ocean. Thus, during 2018, a total of

102 flakes were recorded amongst 3611 silk samples, with each silk filtering about 3 m^3 of seawater. This is equivalent to a mean concentration of about 0.01 paint flakes per m^3, assuming that all non-fibrous microplastics are paint-based, and compares with an estimated concentration of about 0.16 microplastic fibres per m^3. It must be appreciated that both estimates are subject to uncertainty because of constraints on silk efficiency (Richardson et al., 2006) and, with respect to flakes, underestimation because of difficulties in their identification, the existence of finer particles that evade capture and the negative buoyancy of most paint formulations. Regarding size distribution, for example, Kang et al. (2015) found a two-order of magnitude increase in paint particle abundance off the Korean coast when a 330 μm Mantra net was replaced with a 50 μm hand net. Nevertheless, the observations of this study add to the emerging literature in the area suggesting that paint particles represent a significant, yet understudied fraction of the microplastic stock suspended in the ocean (Dibke et al., 2021; Gaylarde et al., 2021).

Acknowledgements

The CPR analysts at the Continuous Plankton Recorder Survey are thanked for providing the microplastics for the study. Funding that supports the CPR data collected has come from: the UK Natural Environment Research Council, Grant/Award Numbers NE/R002738/1 and NE/M007855/1; EMFF Climate Linked Atlantic Sector Science, Grant/Award Numbers NE/ R015953/1, DEFRA UK ME-5308 and ME-414135; NSF USA OCE-1657887; DFO CA F5955-150026/001/HAL; NERC UK NC-R8/H12/100; Horizon 2020; 862428 Atlantic Mission, IMR Norway, DTU Aqua Denmark and the French Ministry of Environment, Energy, and the Sea (MEEM).

415

416 **References**

417 Aliabad, M.K., Nassiri, M., Kor, K., 2019. Microplastics in the surface seawaters of
418 Chabahar Bay, Gulf of Oman (Makran coasts). Marine Pollution Bulletin 143, 125-
419 133.

420

421 Bagaev, A., Mizyuk, A., Khatmullina, L., Isachenko, I., Chubarenko, I., 2017.
422 Anthropogenic fibres in the Baltic Sea water column: Field data, laboratory and
423 numerical testing of their motion. Science of the Total Environment 599-600, 560-
424 571.

425

426 Booher, L.E., 1988. Lead exposure in a ship overhaul facility during paint removal.
427 American Industrial Hygiene Association Journal 49, 121-127.

428

429 Brockenbrough, R.L., 2009. Highway Engineering Handbook, Third Edition.
430 McGraw Hill, New York.

431

432 Burkhardt-Holm, P., N'Guyen, A., 2019. Ingestion of microplastics by fish and other
433 prey organisms of cetaceans, exemplified for two large baleen whale species. Marine
434 Pollution Bulletin 144, 224-234.

435

436 Cardarelli, N.F., 1976. Controlled Release Pesticide Formulations. CRC Press, Boca
437 Raton, FL.

438

Cardoza, A.L.P., Farias, E.G.G., Rodrigues-Filho, J.L., Moteiro, I.B., Scandolo, T.M., Dantas, D.V., 2018. Feeding ecology and ingestion of plastic fragments by *Priacanthus arenatus*: What's the fisheries contribution to the problem? Marine Pollution Bulletin 130, 19-27.

Del Amo, B., Romagnoli, R., Deya, C., Gonzalez, J.A., 2002. High performance water-based paints with non-toxic anticorrosive pigments. Progress in Organic Coatings 45, 389-397.

Dibke, C., Fischer, M., Scholz-Böttcher, B.M., 2021. Microplastic mass concentrations and distribution in German Bight waters by pyrolysis−gas chromatography−mass spectrometry/thermochemolysis reveal potential impact of marine coatings: Do ships leave skid marks? Environmental Science and Technology 55, 2285-2295.

do Sul, J.A.I., Costa, M.F., Baletta, M., Cysneiros, F.J.A., 2013. Pelagic microplastics around an archipelago of the Equatorial Pacific. Marine Pollution Bulletin 75, 305-309.

Driscoll, T.R., Carey, R.N., Peters, S., Glass, D.C., Benke, G., Reid, A., Fritschi, L., 2016. The Australian work exposures study: Occupational exposure to lead and lead compounds. Annals of Occupational Hygiene 60, 113-123.

Gaylarde, C.C., Neto, J.A.B., da Fonseca, E.M., 2021. Paint fragments as polluting microplastics: A brief review. Marine Pollution Bulletin 162, 111847.

Hall, F.X., 2006. Lead in a Baltimore shipyard. Military Medicine 171, 1220-1222.

Hann, S., Sherrington, C., Jamieson, O., Hickman, M., Kershaw, P., Bapasola, A., Cole, G., 2018. Investigating options for reducing releases in the aquatic environment of microplastics emitted by (but not intentionally added in) products. Report for DG Environment of the European Commission. ICF, London.

Herrera, A., Ŝtindlová, A., Martínez, I., Rapp, J., Kutzner-Romero, V., Samper, M.D., Montoto, T., Aguiar-González, B., Packard, T., Gómez, M., 2019. Microplastic ingestion by Atlantic chub mackerel (*Scomber colias*) in the Canary Islands coast. Marine Pollution Bulletin 139, 127-135.

Kang, J.H., Kwon, O.Y., Lee, K.W., Song, Y.K., Shim, W.J., 2015. Marine neustonic microplastics around the southeastern coast of Korea. Marine Pollution Bulletin 96, 304-312.

Lacerda, A.L.d.F., Rodrigues, L. dos S., van Sebille, E., Rodrigues, F.L., Ribeiro, L., Secchi, E.R., Kessler, F., Proietti, M.C., 2019. Plastics in sea surface waters around the Antarctic Peninsula. Scientific Reports 9, 3977.

Lee, H., Lee, D., Seo, J.M., 2021. Analysis of paint traces to determine the ship responsible for a collision. Scientific Reports 11, 134.

Lima, A.R.A., Costa, M.F., Barletta, M., 2014. Distribution patterns of microplastics within the plankton of a tropical estuary. Environmental Research 132, 146-155.

Lindgren, J.F., Ytreberg, E., Holmqvist, A., Dahlström, M., Dahl, P., Berglin, M., Wrange, A.L., Dahlström, M., 2018. Copper release rate needed to inhibit fouling on the west coast of Sweden and control of copper release using zinc oxide. Biofouling 34, 453-463.

Liu, P., Zhan, X., Wu, X.W., Li, J.L., Wang, H.Y., Gao, S.X., 2020. Effect of weathering on environmental behavior of microplastics: Properties, sorption and potential risks. Chemosphere 242, 125193.

Maes, T., Van der Meulen, M. D., Devriese, L. I., Leslie, H. A., Huvet, A., Frère, L., Robbens, J. and Vethaak, A. D., 2017. Microplastics baseline surveys at the water surface and in sediments of the North-East Atlantic. Frontiers in Marine Science 4, doi:10.3389/fmars.2017.00135.

Ng, K.L., Obbard, J.P., 2006. Prevalence of microplastics in Singapore's coastal marine environment. Marine Pollution Bulletin 52, 761-767.

Richard, H., Carpenter, E.J., Komada, T., Palmer, P.T., Rochman, C.M., 2019. Biofilm facilitates metal accumulation onto microplastics in estuarine waters. Science of the total Environment 683, 600-608.

512 Richardson, A.J., Walne, A.W., John, A.W.G., Jonas, T.D., Lindley, J.A., Sims,
513 D.W., Stevens, D., Witt, M., 2006. Using continuous plankton recorder data. Progress
514 in Oceanography 68, 27-74.
515
516 Ruble, D., 2002. Weight loss versus coating density as a measure of applied coating
517 cost. Metal Finishing 100, 53-58.
518
519 Ruiz-Orejon, L.F., Sarda, R., Ramis-Pujol, J., 2016. Floating plastic debris in the
520 central and western Mediterranean Sea. Marine Environmental Research 120, 136-
521 144.
522
523 Sadri, S.S., 2015. Investigation of microplastic debris in marine surface waters using
524 different sampling methods. PhD Thesis, University of Plymouth.
525
526 Song, Y., Hong, S., Jang, M., Kang, J.H., Kwon, O.Y., Han, G.M., Shim, W.S., 2014.
527 Large accumulation of micro-sized synthetic polymer particles in the sea surface
528 microlayer. Environmental Science and Technology 48, 9014–9021.
529
530 Soroldoni, S., Castro, Í.B., Abreu, F., Duarte, F.A., Choueri, R.B., Möller, O.O.,
531 Fillmann, G., Pinho, G.L.L., 2018. Antifouling paint particles: Sources, occurrence,
532 composition and dynamics. Water Research 137, 47-56.
533
534 Takahashi, C.K., Turner, A., Millward, G.E., Glegg, G.A., 2012. Persistence and
535 metallic composition of paint particles in sediments from a tidal inlet. Marine
536 Pollution Bulletin 64, 133-137.

Tanhua, T., Gutekunst, S.B., Biastoch, A., 2020. A near-synoptic survey of ocean microplastic concentration along an around-the-world sailing race. PLOS ONE 15, e0243203.

Thompson, R.C., Olsen, Y., Mitchell, R.P., Davis, A., Rowland, S.J., John, A.W.G., McGonigle, D., Russell, A.E., 2004. Lost at sea: Where is all the plastic? Science 304, 838.

Turner, A., 2017. In situ elemental characterisation of marine microplastics by portable XRF. Marine Pollution Bulletin 124, 286-291.

Turner, A., 2021. Paint particles in the marine environment: An overlooked component of microplastics. Water Research X 12, 100110.

552